sustainability

MDPI

Article

Gully Erosion Induced by Snowmelt in Northeast China: A Case Study

Jinzhong Xu [1,2], Hao Li [3], XiaoBing Liu [3], Wei Hu [3], Qingnan Yang [2], Yanfang Hao [2], Huaicai Zhen [3] and Xingyi Zhang [3,*]

1 College of Forestry, Northeast Forestry University, Harbin 150040, China; xujinzhong@iga.ac.cn
2 Institute of Soil and Water Conservation, Heilongjiang Province Hydraulic Research Institute, Harbin 150080, China; luzhang@bjfu.edu.cn (Q.Y.); haoyanfang@mail.bnu.edu.cn (Y.H.)
3 Northeast Institute of Geography and Agroecology, Chinese Academy of Sciences, Harbin 150081, China; lihao@iga.ac.cn (H.L.); liuxb@iga.ac.cn (X.L.); huwei@iga.ac.cn (W.H.); zhenhuaicai@iga.ac.cn (H.Z.)
* Correspondence: zhangxy@iga.ac.cn; Tel.: +86-451-86602925

Received: 25 February 2019; Accepted: 2 April 2019; Published: 8 April 2019

Abstract: Gully erosion stands out as one of the worst aspects of farmland degradation, which induces the loss of arable soil and tractor operation. Most of the gully erosion studies focused on the influence of precipitation erosion, slope erosion, and the freeze–thaw cycle on soil characteristics. Few studies discussed the effect of snowmelt on gully development. In this paper, the gully development induced by snowmelt was observed in a typical gully in Hailun City, the center of the Mollisols area of northeast China. The results showed that, during the snow melting period of 2017, the soil loss induced by snow melting was 0.22 t at the gully head + 0 m, 14.27 t at the gully head + 77 m, and 7.63 t at the gully head + 239 m, while 98.1% of the sediment was from the gully erosion. The horizontal projected area of the observed gully increased by 56.96 m^2, and the gully head advanced 2.3 m during the snow melting period. About 92.2% of the total runoff occurred in the initial snow melting period. The discharge runoff and sediment concentration had a significant correlation with the air temperature above 0 °C, and the same relationship existed between the discharge runoff and sediment concentration in the initial and middle snowmelt stages. The results indicate that the gully development induced by snowmelt should not be ignored in the area.

Keywords: Mollisols; gully erosion; snowmelt; runoff and sediment; gully development; northeast China

1. Introduction

Gully erosion is recognized as a major and the most serious form of land degradation [1,2], which is one of the main sources of sediment yield [3]. The majority of research on gully erosion in the past century focused on the importance, main processes, influencing factors and its detrimental effects [4,5]. Gully erosion is not a homogeneous process. It is triggered or accelerated by multiple driver factors, such as hydraulic, wind, snowmelt, freeze–thaw cycle, gravity, and field management [6,7]. Although anthropic influence is typically the main driver of gully erosion evolution [5], surface water flow of catchment is the prime and dominant force of gully development [8]. Undoubtedly, the evaluation of the impact of water flow on gully development is the most popular approach in gully erosion literature [9]. Snowmelt processes contribute part of the water flow to gully erosion in high latitude areas and cold regions [10,11]. Previous research indicated that the erosion rate of snowmelt can reach or surpass that of precipitation [12].The sediment transport caused by snowmelt runoff accounts for 76% of the total yield in the Schafertal Basin in eastern Germany [13]), 80% in the Peace River Basin of British Columbia [14], 90% along the Pacific coast of the northwestern United States [15], and 96% in Fosheim Peninsula of Canada [16].

As one of the four continuous areas of the world [17], the Mollisols in northeast China was seriously degraded by gully erosion. Gully erosion has become the dominant driving factor of soil degradation in the region [18]. The ground in the area is usually covered by snow from November to March [19], with snowfall accounting for 7% to 25% of the total annual precipitation [20]. During the snow melting period, most of the farmland was without residual cover, and very thin top soil was thawed and saturated, which increased the surface runoff and soil loss. Therefore, the initiation and development of gullies in this area due to surface water flow were not only from rainfall but also from snowmelt [21,22]. However, snowmelt erosion, specifically the impact of snowmelt erosion on variations in gully erosion, is rarely investigated.

In this paper, a typical gully erosion was observed, and the characteristics of the gully development induced by snowmelt were identified in the Mollisols area of northeast China. Our objective was to understand the seriousness of the gully erosion, to investigate the characteristics of the gully development due to snowmelt in this region. The findings will guide land managers to implement several land-use strategies.

2. Materials and Methods

2.1. Site Description

The catchment is located in the center of the Mollisols area of northeast China, at the Guangrong Soil and Water Monitoring Station of the Chinese Academy of Sciences in Hailun City, Heilongjiang Province (47°23′ north (N), 126°51′ east (E)). The study site belongs to the north temperate zone with a continental monsoon climate. It is cold in winter with northwest wind, but hot and rainy in the summer with heavy rainfall. The annual mean precipitation is 530 mm, with 65% occurring in June to August with an average precipitation of 472 mm from March to October. The annual mean temperature is 1.5 °C. A monthly average temperature below 0 °C occurs from November to March, with a typical mean minimum temperature of −37 °C. The air temperature often rises above 0 °C in mid-March, and the snow begins to melt in late March. The annual average snow fall is about 50 mm [23].

The observed gully was in a north-to-south slope land, and was initially cultivated in 1942, while the south zone was reforested in 2007 [24]. The initial gully formation was identified in a satellite remote sensing image since 1960 [25]. Up to the year of 2017, the horizontal projected area of the observed gully was 3011.3 m^2 with a length of 239 m. The gully consists of an active and a stable sub-area. The active sub-area is positioned in the upper zone, with an area of 1174.3 m^2—77.2 m long and a mean width of 15.2 m. An ephemeral gully was formed on the upslope, with a length of 173 m and a distance of 11 m from its headcut to the watershed. In order to differentiate the components of the surface runoff and sediment transportation, the catchment area (Figure 1) was divided into several catchment zones (Table 1).

Table 1. The basic information of the catchment and its subzones.

	Area (ha)	Average Slope Steepness (°)	Land Use
Zone A	3.27	3.0	Cultivated
Zone B1	0.59	2.5	Cultivated
Zone B2	0.69	2.2	Cultivated
Zone C1	0.41	4.6	Reforest
Zone C2	0.44	4.0	Reforest
Total	5.70		

The cultivated land was ridged along the contour line by tractor in each autumn or spring. The ridge was 20 cm high and 70 cm wide. The ridge direction almost crossed the gully line. The soil is typical of the Mollisols with high organic matter content. Soil properties in the different soil layers in the catchment are given in Table 2.

Table 2. Soil properties in the observed site.

Soil Layers (cm)	SOM (g/kg)	Soil Shear Strength (kPa)	Water Stable Aggregate		Soil Texture
			MWD (mm)	GMD (mm)	
0–10	39.4	4.8	2.89	1.23	Loamy clay
10–20	25.8	23.7	3.99	1.51	Clay loam
20–30	21.6	14.1	1.11	0.79	Silty clay
50–60	13.8	5.8	1.89	0.99	Sandy clay
150–160	12.4	5.4	0.66	0.70	Loamy clay
250–260	3.5	3.5	0.53	0.58	Loamy clay
350–360	4.6	3.2	0.70	0.68	Clay
450–460	4.7	3.6	0.43	0.60	Clay

MWD = mean weight diameter (mm); GMD = geometry mean diameter (mm).

Figure 1. The gully catchment and the location of Thomson V-notch weir.

2.2. *Snow Measurement*

The mass and spatial distribution of snow on the ground varied during winter time, and the amount of snowmelt was dominantly determined by the depth and bulk density [26]. The snow in the catchment was observed using the grid method. The snow depth and density of 67 sites in total in the catchment were measured (Figure 2). The snow depth was measured directly using a steel ruler with an accuracy of 1 mm. Meanwhile, the snow samples were collected using a metal cylinder with a diameter of 15.5 cm and they were weighed using an electronic scale with an accuracy of 0.01 g. The snow bulk density was calculated based on snow weight and volume.

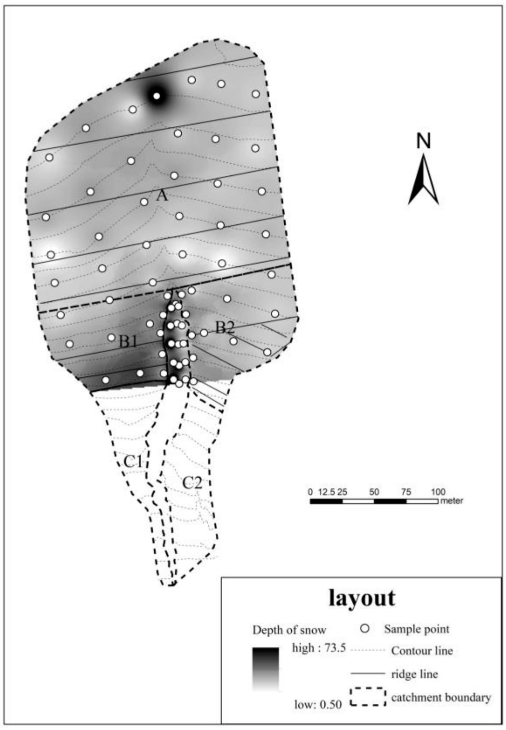

Figure 2. The points of snow sample collections.

2.3. Snowmelt Runoff Observation

The surface runoff flow is a dominant driving force in gully development. The iron sheet barrier with a Thomson V-notch weir [26,27] was fixed on the bottom of the gully head + 0 m, gully head + 77 m (the boundary between the active and stable sub-area), and gully head + 239 m (Figure 1). The runoff was filled in a collecting bucket, and flow rate was manually measured every hour from 9:00 a.m. to 6:00 p.m. daily during the snow melting period, while the runoff samples were collected using a sampling bottle (500 mL) for sediment concentration measurement [28]. In total, 242 samples in three observation sites (gully head + 0 m; gully head + 77 m; gully head + 239 m) were collected. No observations were performed at night, because it was freezing cold and there was no runoff available.

The formula for calculating the total runoff Tr is as follows:

$$Tr = \sum({}_i \times Dr_i), \tag{1}$$

where $_i$ (m^3/s) is the flow rate at the i-th hour during the snow melting period, and Dr_i (second) was set as 3600 s.

2.4. Sediment Concentration Measurement

About 500 mL of runoff sample was collected from the collecting bucket after it was evenly stirred. The collected samples were left to stand for 24 hours, and then supernatant was removed. The weight of sediment was measured using the oven-drying method. The sediment concentration was calculated using the equation [29] below.

$$C_s = (W_{b+s} - W_b)/V, \tag{2}$$

where C_s is the sediment concentration of the water sample (g/L), W_{b+s} is the total weight of the sampling bottle and sediment (g), W_b is the weight of the sampling bottle (g), and V is the volume of the runoff sample (L). The total sediment yield was calculated with the sediment concentration and the amount of runoff.

$$Ts = \sum(Cs_i \times hr_i) = \sum(Cs_i \times i \times 3600\ s), \tag{3}$$

where Cs_i (g/L) is the sediment concentration at the i-th hour during the snow melting period, hr_i is the runoff discharge at the i-th hour during the snow melting period, and i (second) was set as 3600 s.

2.5. Spatial Measurement

The topography of the catchment and horizontal variation of the observed gully were measured using an unmanned airborne vehicle (UAV) combined with ground control points. The method is a non-invasive field and high-speed measurement [30] with high spatial resolution [31,32], which is widely applied in the studies of denudation and sedimentation [33,34]. The topography of the catchment and the gully was measured using the UAV DJI inspire2 (Shenzhen, China) drone equipped with a one-inch complementary metal–oxide–semiconductor (CMOS) sensor with effective pixels of 20 MP (Camera model FC6310) to collect images combined with six ground control points two times. The first time was on 24 October 2016 before snow; the second time was on 28 March 2017 for the gully after snow melting. The three-dimensional information of the six ground control points was accurately measured using a Real-Time Kinematic (RTK-GPS, Yinhe 6, China). The flight height was 10 m and the image overlap rate was 70% [35,36]. The image data and RTK measured data were processed and converted to digital surface model (DSM) data using the Pix4Dmapper software (Pix4D, EPFL, Lausanne), and overlap analysis of the digital surface model was conducted using ArcGIS 10.3 (ESRI, Redlands, CA, USA). A digital topographic map with 1.0-cm resolution of the catchment was created. The topographic data were used to plot catchment areas. The horizontal variation of the observed gully was analyzed. Observation error among three coordinate directions X, Y, and Z was 0.3 cm, 2.3 cm, and 1.6 cm, respectively.

2.6. Meteorological Data

The main meteorological data—the air and ground surface temperatures, and wind velocity and direction—were monitored in a micro weather station and geothermometer (AMS-IV, China).

3. Results and Analysis

3.1. Spatial Distribution of Snow Cover in the Watershed

The snow mass and its spatial distribution was measured on 24 February 2017, based on the snowfall and maximum snow mass covered on the ground in the catchment during the winter before snow melting [37]. Significant spatial heterogeneity of snow thickness both in the slope of the catchment and gully was observed. The average snow thickness on the slope was 20.9 cm, 18.4 cm in the east slope farmland of the gully, and 23.4 cm in the west slope farmland of the gully. The mean snow thickness in the gully was 39.6 cm on the bottom, 63.4 cm on the west slope side, 0.4 cm on the east slope side, 28.9 cm on the 2-m bank to the west gully edge line, and 20.9 cm on the 2-m bank to the east gully edge line. During the winter from November 2016 to March 2017 before snow melting in the study site, the hourly average wind velocity at the height of 10 m was 1.7 m/s, and the maximum wind speed was 17.3 m/s, while the mean wind direction was 318° (0 represents the north) (Figure 2). Hence, the covered snow on the ground was moved from northwest to southeast. Much snow deposited and heaped against the forest in the south boundary of zone B1. When the removed snow drifting by wind from northwest to southeast reached the west slope wall of the gully, the snow slid down and heaped along the west slope wall of the gully. The west slope wall of the gully was covered by much deeper snow, whereas no removed snow could reach the east slope wall of the gully. Furthermore, the snowfall slid down along the east slope wall. As a result, the snow cover on the east slope wall of the gully was considerably lower (only 0.4 cm). A point of thick snow cover appeared in the head of the ephemeral gully, which might be due to willow vegetation. The observed snowfall was 31.9 mm in the observed winter, and on 24 February 2017, 0.8 mm of snowfall occurred after the snow observation. Converting the snowfall to water amount, it was approximately 1818 m^3; however, the observed runoff was 2033 m^3 of water in the catchment area of the gully. This means that an extra 215 m^3 of snow was blown from other areas to the gully catchment.

3.2. Snowmelt Runoff to Gully

Normally, the gully is mostly accelerated by a hydraulic factor. It was proven that the snowmelt runoff is as important as the runoff derived from rainfall for the gully development [27]. The total runoff during the snow melting period was 396.5 m^3 at gully head + 0 m, 619 m^3 at gully head + 77 m, and 960.3 m^3 at gully head + 239 m (Table 3). The 396.5 m^3 of runoff at gully head + 0 m was from the gully head catchment, zone A. Its runoff coefficient was 38.4%. The runoff from zones B1 and B2, and the gully body corresponding to zone B1 was 222.5 m^3, and its runoff coefficient was 23.9%. The runoff from zones C1 and C2, and the gully body corresponding to zone C1 was 341.3 m^3.

Table 3. Daily runoff and sediment transportation at different sites in the gully.

	Gully Head + 0 m		**Gully Head + 77 m**		**Gully Head + 239 m**	
	Runoff (m^3)	**Sediment (kg)**	**Runoff (m^3)**	**Sediment (kg)**	**Runoff (m^3)**	**Sediment (kg)**
15 March	115.0	24.6	111.8	1152.9	187.3	689.4
16 March	128.7	158.9	202.4	1274.9	339.7	927.4
17 March	138.4	0.0	256.6	10,235.6	358.9	4902.3
18 March	9.8	36.0	13.1	389.2	27.3	440.9
19 March	3.6	1.2	12.7	477.7	19.7	430.8
20 March	0.7	0.4	7.2	245.5	9.7	93.4
21 March	0.3	0.0	5.4	185.5	6.7	58.8
22 March	-	-	2.3	41.7	3.3	24.7
23 March	-	-	1.9	49.1	2.2	16.6
24 March	-	-	2.1	88.6	2.2	26.2
25 March	-	-	1.6	71.3	1.4	10.5
26 March	-	-	1.2	33.8	1.3	4.9
27 March	-	-	0.7	22.5	0.6	2.1
Total	396.5	221.1	619.1	14,268.2	960.3	7627.9

The driving force of water flow on gully depended on not only the mass but also the runoff discharge. The observation showed that the discharge runoff changed a lot with the stages of daily snowmelt. The duration of the snowmelt runoff was from 15 March to 27 March in the spring of 2017. Based on the daily maximum discharge runoff, the snow melting period was divided into the initial stage (15–17 March), middle stage (18–22 March), and final stage (23–27 March). The dynamic of daily discharge runoff at each observation site displayed a single-peak curve. The initial runoff occurred on 15 March, at 10:11 a.m. at gully head + 0 m, 10:17 a.m. at gully head + 77 m, and 10:18 a.m. at gully head + 239 m. The air temperature above 0 °C appeared from 10:00 a.m. to 8:15 p.m., and the maximum air temperature occurred at 4:05 p.m. The peak discharge flow happened at 5:00 p.m., and it was 6.73 L/s at gully head + 0 m, 9.93 L/s at gully head + 77 m, and 13.2 L/s at gully head + 239 m. The dynamic of discharge runoff during the snow melting period at each observation site showed a left-skewed single-peak curve. The peak discharge flow appeared on the third day, 17 March, when the daily maximum and mean air temperature reached 8.2 °C and 4.7 °C, respectively. The daily dynamic relationship between discharge runoff and daily air temperature above 0 °C is shown in Figure 3.

It was found that 92.2% of the total runoff occurred in the initial stage of the snow melting period, whereas 6.6% occurred in the middle stage and 1.2% occurred in the final stage. The maximum discharge flow was 10.2 L/s at gully head + 0 m,16.3 L/s at gully head + 77 m, and 17.8 L/s at gully head + 239 m (Figure 3).

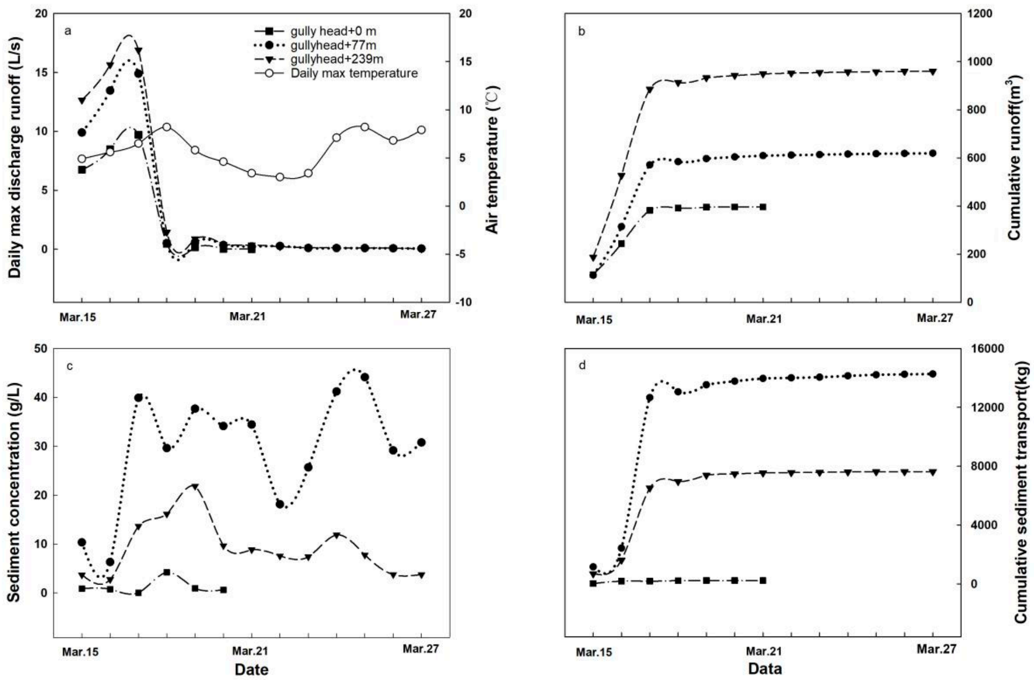

Figure 3. Runoff and sediment transportation processes during the snow melting period: (**a**) daily maximum discharge runoff; (**b**) cumulative runoff; (**c**) average daily sediment concentration; (**d**) cumulative sediment transportation.

3.3. Snow Melting Sediment Transportation of Gully

The sediment transportation revealed the intensity of soil erosion [38]. The gully erosion induced by snowmelt could be identified by the sediment transportation at the three observation sites. The total sediment transportation during the snow melting period was 0.22 t at gully head + 0 m, 14.27 t at gully head + 77 m, and 7.63 t at gully head + 239 m (Table 3). The 0.22 t of sediment transportation at gully head + 0 m was from the gully head catchment, zone A. The maximal sediment transportation was at gully head + 77 m. The sediment came from the 4.55-ha slope farmland of zones A, B1, and B2, and the area of 1174.3 m^2 of the gully body corresponding to the zone B1. The soil loss induced by snowmelt was 14.27 t. However, 98.1% of the sediment was from the gully erosion. This result indicated that gully erosion was the dominant phenomenon caused by snowmelt erosion in the observation area. Compared to the position at gully head + 77 m, the sediment transportation at gully head + 239 m decreased by half. The reasons were as follows: firstly, almost no sediment was added because zones C1 and C2 were covered either by forest or by natural withered grasses in the stable gully section (Figure 2); secondly, the slope steepness and the length of the gully bottom corresponding to the active and stable section of the gully were 8.4% and 77 m, and 1.4% and 162 m, respectively; thirdly, the gully surface was undulated and bare in the active section, but relatively gentle and vegetative in the stable section. Those factors decreased the velocity of the runoff flow and induced more sediment sinking on the bottom of the gully in the stable section. The soil loss induced by snowmelt was 7.63 t.

The dynamic of the daily sediment concentration (d) at each observation site displayed a similar curve to the daily discharge runoff. However, the maximal sediment concentration was about one hour later than the maximal discharge runoff (Figures 3 and 4). The sediment concentrations were low in the initial stage, and markedly increased in the middle stage of snowmelt. The ground surface was covered by snow and the top soil was frozen in the initial snow melting stage, while not much soil was transported by runoff flow. With the increase in daily temperature and discharge runoff, a thin layer of top soil was thawed, and the sediment concentration and transportation increased in the middle stage of snowmelt. The highest sediment concentration was found at gully head + 77 m in the final stage (Figure 3). This can be explained by the fact that the soil collapsed from the gully wall and head, and rolled down into the runoff flow on the gully bottom, which greatly increased the sediment concentration.

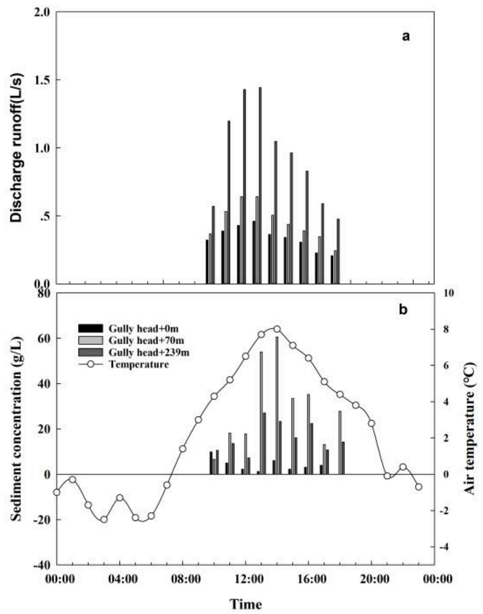

Figure 4. Daily variations of the discharge runoff and sediment concentration at the three observed sites in the day of 18 March 2017: (**a**) hourly discharge runoff; (**b**) hourly sediment concentration.

As shown above, 92.2% of the total runoff occurred in the initial stage of snowmelt, while the sediment yield at gully head + 0 m, gully head + 77 m, and gully head + 239 m accounted for 83.0%, 88.8%, and 85.5% of the total sediment yield in the same stage, respectively (Table 3).

4. Discussion

4.1. Snow Redistribution

In high latitude areas of the earth, snow usually covers the ground in the winter [39], and the snow depth is around 30 cm to 50 cm in the coldest period. In the study area, the majority of the snow falls during the period from December to February, and the snow distribution on the ground is generally determined by wind direction and landscape [40].

The catchment of the observed gully is north–south slope land. The altitude intercept between the highest point in the center of the north line and the lowest point in the center of the south line was 29.9 m. The length of the catchment from north to south was 423 m, while the average width from west to east was 134.8 m. The land-use type of the catchment can be divided into two sub-areas. The sub-area in the north is farmland, and it is ridged from west to east. The south sub-area was reforested in the year of 2007. The gully formed in the middle low zone of the catchment (Figure 1). The snow drifted along the wind direction and deposited on the slope depending on the landscape changes. The moving snow (88 mm in total) was intercepted and sunk in front of the forest., which was about 2.7 times more than that in the zone B1. When the wind-moved snow reached the west bank of the gully, the snow continually rolled down and thickened the west slope side of the gully. At the same time, the snow fell on the east side of the gully, rolled down, and blew away. The consequences were 122 mm of snow cover on the west side of the gully, and nearly no snow on the east side of the gully. This indicates that slope land snow distribution is also strongly influenced by wind direction and landscape.

4.2. Runoff and Sediment Transportation Processes under the Snowmelt

The processes of runoff and sediment transportation were differently induced by rainfall and snowmelt, especially for the gully erosion [5,41]. The runoff event characteristics governed by the contribution of snowmelt and the seasonality of the aridity index was non-negligible in high latitudes of the northern hemisphere [42]. The rainfall runoff and sediment transportation were random events, determined by precipitation intensity and soil infiltration rate [43]. Snowmelt runoff and sediment transportation were events determined by air temperature and snow mass. The snowmelt runoff happened during the day time when air temperature was above 0 °C, but stopped and refroze at night when air temperature was below 0 °C. The temperature directly affects the flow rate (Figure 4) and thawing depth of soil, which then affects sediment transport. In the initial stage of snowmelt on 15 March, the first day of the snowmelt, the melted snow was mainly from the ridge top and brought little sediment to the furrow. A macropore meltwater flow drained slowly in the saturated soil snow along the slope of ridge direction. On the second day (16 March), the meltwater flow flew onto the ice layer. The discharge runoff increased with the increase in air temperature. However, there was almost no sediment transportation because of the meltwater from the furrow moving onto the frozen layer, which did not touch the soil. On the third day (17 March), the discharge runoff reached the largest point, and the sediment transportation increased markedly, which resulted in the most serious day of gully erosion. More than 90% of total runoff and 80% of total sediment transportation occurred in the first stage of snowmelt. As a result, the gully head was cut, and the gully wall collapsed and expanded due to the stream of meltwater. The middle stage of snowmelt was from 18 March to 22 March, and the runoff in the catchment of the gully head ended on 21 March. Only 3.6% of total runoff and 17.0% of total sediment transportation occurred in this stage. The duration of snowmelt was one week, the same as reported by a previous study [23]. The runoff and sediment transportation decreased significantly in the middle stage of snowmelt, and the total runoff and total sediment transportation were 6.6% and 9.4% at the gully head + 77 m, and 6.9% and 13.7% at the gully + 239 m. The runoff mainly came from the snow which sunk and stored in the gully. The sediment concentration maintained a higher level due to the gully erosion (Figure 3). Although the runoff in the gully continued another five days in the final stage of snowmelt, the discharge runoff and sediment transportation were very low, and there was almost no gully erosion in this stage (Figure 3).

The dominant driving force of gully erosion is the hydraulic power [44]. The intensity of gully erosion during the snowmelt could be demonstrated by the discharge runoff and sediment concentration. Except for the mass of snow covering the ground, the discharge runoff was determined by the air temperature. Our observation results showed that the discharge runoff and sediment concentration had significant correlation ($p < 0.05$) with air temperature above 0 °C in the initial and middle stages of snowmelt. Meanwhile, there was also a significant correlation ($p < 0.05$) between discharge runoff and sediment concentration in the same stage (Table 4).

Table 4. Analysis of the correlations among the hourly discharge runoff, sediment concentration, and air temperature.

Indicator	Sediment Concentration	Air Temperature	Date
Discharge runoff	0.47 *	0.71 **	15 to 17 March
	0.32 *	0.74 **	18 to 22 March
	0.24	−0.22	23 to 27 March
Sediment concentration	1	0.63 **	15 to 17 March
	1	0.36 *	18 to 22 March
	1	0.18	23 to 27 March

* $p < 0.05$; ** $p < 0.01$.

4.3. Gully Development Induced by Snowmelt

As a result of snowmelt erosion, the gully significantly developed in the gully head and gully bank in the active section. These could be directly revealed by the changes in gully area and gully head advancement. The variation of the gully before and after snowmelt was recorded by UAV. The horizontal area of the gully was increased by 56.96 m^2 during the snowmelt. Two active areas were found. One was the gully headcut development, which was advanced by 2.3 m. It had an average horizontal area of 22.28 m^2 and a volume of 3.68 m^3. It was eroded by the stream coalesced runoff from the catchment of the gully head. A sink hole of 42 cm in diameter and 145 cm in depth was found in front of the gully head before snowmelt. It connected to the original gully head to form an underground path. The meltwater flew into the hole and enlarged it. The hole was collapsed on the third day of snowmelt. The concentrated snowmelt runoff continually scoured the bare soil in the headcut and deepened the gully head bottom by falling flow [45]. Another factor was the gully bank expansion, which happened on both sides of the gully in the active section (Figure 5). There were many fissures induced by frost heave along the gully bank. The soil body between the fissure and gully boundary glided down when the meltwater went into the fissures and thawed the deeper layer of soil. The sidewall collapsed with the combined effect of the water, the freeze–thaw cycle, and gravity. Our observation showed that most of the gully slope erosion occurred on the leeward gully bank, where the snow thickness was significantly greater than the average snow thickness. Several soil bodies with a width of 20 cm to 40 cm closer to the gully boundary slid down about half a meter. The topsoil conditions of the gully slope varied from ice- and snow-covered surface to thawed surface with frozen subsoil, whereby some sheet erosion and rill erosion occurred on the gully slope because snowmelt water and frozen soil restricted infiltration. Firstly, a channel cut develops through the topsoil of gully slope, and the second stage begins when the rill penetrates downward into the weaker subsoil [46]. Sediment was transported into the gully bottom through discharge. This is a typical phenomenon of gully side expansion, which increased the gully area by 34.68 m^2. The gully bottom was not cut by meltwater flow in the active section, but deposited in the stable section. Most studies indicated that soil erodibility was higher during the thawing of soil in March–April, which was 2–3 times higher than that during other periods [47]. The frozen layer restricted water infiltration, which resulted in increases in the surface runoff and soil water content and, therefore, increased erosion [48]. When the snowmelt runoff flew down along the bare surface of the steep gully wall, the thawed surface soil was lost, and some larger soil clods collapsed. The incompletely thawed layer was the main reason for the occurrence of large-range sheet erosion and small rill erosion [46]. The frozen layer made the snowmelt water easier to concentrate and facilitated the capacity to cause scour, while the thawing depth of the soil had a significant influence on the erosion process [49].

In this study, we did not consider the combination effect of rainfall and snowmelt on gully erosion, since rainfall was rather seldom in this season. Actually, the gully erosion could be accelerated if rainfall accompanies snowmelt. Research in Norway showed that even a small rain event on frozen ground before snow cover could cause severe rill and ephemeral gully erosion, especially when the soil has high silt content [50].

In our research, the gully bank and headcut retreat occupied 60% and 40% of the gully development area, respectively; this demonstrates that they are the risky processes and, thus, need conservation measurements. Similar to rainfall-induced gully erosion, resulted sidewall collapse at the base of channel wall was the main reason for gully bank retreat. Therefore, one approach for gully reclamation is to grade the channel bank to a steepness such as a 2 (horizontal):1 (vertical) ratio and establish grass vegetation that can resist the erosive forces of the flow. Given the highly fertile black soil, the willow trees are usually planted to increase resistance to high velocities along the steam banks. For headcut retreat, drop structures that reduce the energy grade along a channel can be used to protect an overfall [51].

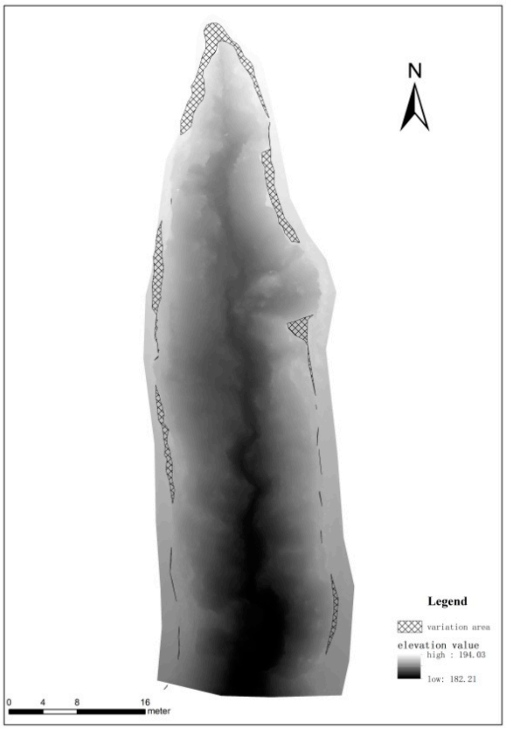

Figure 5. Expansion area of the gully induced by snowmelt erosion.

5. Conclusions

The characteristics and processes of gully erosion due to snowmelt were much different from those due to rainfall in northeast China. In contrast with the random event of rainfall erosion, the snowmelt erosion was determined by air temperature above 0 °C. Normally, it occurred in the daytime, while the snowmelt refroze at night. Because of the existence of the frozen layer, the surface snowmelt runoff coefficient was much higher than the rainfall runoff coefficient. However, the soil loss for the slope snowmelt erosion was relatively lower than that for rainfall. Except for the land use and topography, the rainfall erosion was mainly determined by rainfall intensity and its duration, whereas the snowmelt erosion was greatly impacted by air temperature—the higher air temperature was, the larger the discharge runoff was (i.e., more serious gully erosion). One of the most significant characteristics of the snowmelt gully erosion was that most of the runoff and sediment delivery happened in the initial stage of snowmelt period.

The soil loss of the slope snowmelt erosion was 0.22 t at gully head + 0 m, and the soil loss of the gully snowmelt erosion at gully head + 77 m was 14.27 t. More than 98% of the sediment was from the gully erosion. The snowmelt erosion greatly impacts gully erosion, but not so much the slope erosion in northeast China.

Author Contributions: J.X. and X.Z. designed the research. J.X., H.L., H.Z. and W.H. implemented the research, J.X., Q.Y. and Y.H. analyzed the data and the results, J.X., X.Z. and X.L. wrote and revised the manuscript together.

Funding: This research was funded by the National Key R&D Program of China grant number [2017YFC0504200] and the National Natural Science Foundation of China grant number [41601289]. And The APC was funded by [2017YFC0504200].

Acknowledgments: The data supported by the "Scientific Data Center of Northeast Black Soil, National Earth System Science Data Sharing center of China (http://northeast.geodata.cn)" are appreciated.

Conflicts of Interest: The authors declare no conflict of interest.

References

1. Dotterweich, M.; Rodzik, J.; Zgłobicki, W.; Schmitt, A.; Schmidtchen, G.; Bork, H.R. High resolution gully erosion and sedimentation processes, and land use changes since the Bronze Age and future trajectories in the Kazimierz Dolny area (Nałęczów Plateau, SE-Poland). *Catena* **2012**, *95*, 50–62. [CrossRef]
2. Pimentel, D.; Burgess, M. Soil erosion threatens food production. *Agriculture* **2013**, *3*, 443–463. [CrossRef]
3. Krause, A.K.; Franks, S.W.; Kalma, J.D.; Loughran, R.J.; Rowan, J.S. Multi-parameter fingerprinting of sediment deposition in a small gullied catchment in SE Australia. *Catena* **2003**, *53*, 327–348. [CrossRef]
4. Poesen, J. Challenges in gully erosion research. *Landf. Anal.* **2011**, *17*, 5–9.
5. Castillo, C.; Gómez, J.A. A century of gully erosion research: Urgency, complexity and study approaches. *Earth Sci. Rev.* **2016**, *160*, 300–319. [CrossRef]
6. Parkner, T.; Page Mike, J.; Marutani, T.; Trustrum, N.A. Development and controlling factors of gullies and gully complexes, East Coast, New Zealand. *Earth Surf. Process. Landf.* **2006**, *31*, 187–199. [CrossRef]
7. Valentin, C.; Poesen, J.; Li, Y. Gully erosion: Impacts, factors and control. *Catena* **2005**, *63*, 132–153. [CrossRef]
8. Le Roux, J.J.; Sumner, P.D. Factors controlling gully development: Comparing continuous and discontinuous gullies. *Land Degrad. Dev.* **2002**, *23*, 440–449. [CrossRef]
9. Chaplot, V.; Brown, J.; Dlamini, P.; Eustice, T.; Janeau, J.L.; Jewitt, G.; Lorentz, S.; Martin, L.; Nontokozo-Mchunu, C.; Oakes, E.; et al. Rainfall simulation to identify the storm-scale mechanisms of gully bank retreat. *Agric. Water Manag.* **2011**, *98*, 1704–1710. [CrossRef]
10. Golosov, V.; Koiter, A.; Ivanov, M.; Maltsev, K.; Gusarov, A.; Sharifullin, A.; Radchenko, I. Assessment of soil erosion rate trends in two agricultural regions of European Russia for the last 60years. *J. Soils Sediment* **2018**, *18*, 3388–3403. [CrossRef]
11. Sonneveld, M.P.W.; Everson, T.M.; Veldkamp, A. Multi-scale analysis of soil erosion dynamics in Kwazulu-Natal, South Africa. *Land Degrad. Dev.* **2005**, *16*, 287–301. [CrossRef]
12. Demidov, V.; Ostroumov, V.Y.; Nikitishena, I.; Lichko, V. Seasonal freezing and soil erosion during snowmelt. *Eurasian Soil Sci.* **1995**, *27*, 78–87.
13. Ollesch, G.; Kistner, I.; Meissner, R.; Lindenschmidt, K.E. Modelling of snowmelt erosion and sediment yield in a small low-mountain catchment in Germany. *Catena* **2006**, *68*, 161–176. [CrossRef]
14. Vliet, L.J.P.V.; Hall, J.W. Effects of two crop rotations on seasonal runoff and soil loss in the Peace River region. *Can. J. Soil Sci.* **1991**, *71*, 533–543. [CrossRef]
15. Wischmeier, W.H.; Smith, D.D. *Predicting Rainfall Erosion Losses: A Guide to Conservation Planning*; Agriculture Handbook No. 537; US Department of Agriculture: Washington, DC, USA, 1978.
16. Lewkowicz, A.G.; Kokelj, S.V. Slope sediment yield in arid lowland continuous permafrost environments, Canadian Arctic Archipelago. *Catena* **2002**, *46*, 261–283. [CrossRef]
17. Liu, X.; Lee, B.C.; Kravchenko, Y.S.; Duran, A.; Huffman, T.; Morras, H.; Studdert, G.; Zhang, X.; Cruse, R.M.; Yuan, X. Overview of Mollisols in the world: Distribution, land use and management. *Can. J. Soil Sci.* **2012**, *92*, 383–402. [CrossRef]
18. Zhang, Y.G.; Wu, Y.Q.; Wang, Y.Z.; Liu, B.Y. Seasonal discrepancy of ephemeral gully erosion in Northeast China with black soils. *Geogr. Res.* **2008**, *27*, 145–154.
19. Zhang, S.; Xiao, Y.; Zhang, H.; Song, G.; Wang, Q. Influence of three typical forest types on processes of snowfall, snow cover and snow melting in Fenglin National Nature Reserve. *J. Soil Water Conserv.* **2015**, *29*, 37–41.
20. Jiao, J.; Xie, Y.; Lin, Y.; Zhao, D.F. Study on snowmelt runoff and sediment yields in Northeast China. *Geogr. Res.* **2009**, *28*, 333–344.
21. Hu, G.; Wu, Y.; Liu, B.; Yu, Z.; You, Z.; Zhang, Y. Short-term gully retreat rates over rolling hill areas in black soil of Northeast China. *Catena* **2007**, *71*, 321–329. [CrossRef]
22. Li, H. *Gully Erosion Evolvement and Effect in Typical Black Soil Region*; Northeast Institute of Geography and Agroecology: Changchun, China, 2016; pp. 5–9.
23. Wang, P.; Li, H.; Chen, Q.; Chen, S.; Xun, J.Z.; Song, C.Y.; Zhang, X.Y. Different scale observation sites of snow melt runoff in typical black soil area. *Bull. Soil Water Conserv.* **2014**, *34*, 244–253.
24. Zhang, X.Y.; Wang, Q.C.; Sui, Y.Y.; Yu, T.T. Spatial-Temporal variation of soil moisture and its spatial correlations with soybean yield in black soil sloping farmland. *Soils* **2006**, *38*, 410–416.

25. Liu, X.B.; Zhang, X.Y.; Wang, Y.X.; Sui, Y.Y.; Zhang, S.L.; Herbert, S.J.; Ding, G. Soil degradation: A problem threatening the sustainable development of agriculture in Northeast China. *Plant Soil Environ.* **2010**, *56*, 87–97. [CrossRef]
26. Komissarov, M.A.; Gabbasova, I.M. Snowmelt-Induced Soil Erosion on Gentle Slopes in the Southern Cis-Ural Region. *Eurasian Soil Sci.* **2014**, *47*, 598–607. [CrossRef]
27. Rodzik, J.; Furtak, T.; Zglobicki, W. The impact of snowmelt and heavy rainfall runoff on erosion rates in a gully system, Lublin Upland, Poland. *Earth Surf. Process. Landf.* **2009**, *34*, 1938–1950. [CrossRef]
28. Water Conservancy Industry Standard of the People's Republic of China. *Technical Code of Practice on Water and Soil Conservation Monitoring SL277-2002*; Ministry of Water Resources of the People's Republic of China: Beijing, China, 2002.
29. Hua, W.; Fan, H.; Xu, X. Observation on the spring snowmelt erosion og sloping farmland in Northeast China. *J. Soil Water Conserv.* **2017**, *31*, 92–110.
30. Eltner, A.; Mulsow, C.; Maas, H.G. Quantitative measurement of soil erosion from TLS and UAV data. In Proceedings of the International Archives of the Photogrammetry, Remote Sensing and Spatial Information Sciences, Rostock, Germany, 4–6 September 2013; Volume XL-1/W2.
31. Bremer, M.; Sass, O. Combining airborne and terrestrial laser scanning for quantifying erosion and deposition by a debris flow event. *Geomorphology* **2012**, *138*, 49–60. [CrossRef]
32. Bazzoffi, P. Measurement of rill erosion through a new UAV-GIS methodology. *Ital. J. Agron.* **2015**, *10*. [CrossRef]
33. Peter, K.D.; d'Oleire-Oltmanns, S.; Ries, J.B.; Marzolff, I.; Ait Hssaine, A. Soil erosion in gully catchments affected by land-levelling measures in the Souss Basin, Morocco, analysed by rainfall simulation and UAV remote sensing data. *Catena* **2014**, *113*, 24–40. [CrossRef]
34. Neugirg, F.; Stark, M.; Kaiser, A.; Vlacilova, M.; Della Seta, M.; Vergari, F.; Schmidt, J.; Becht, M.; Haas, F. Erosion processes in calanchi in the Upper Orcia Valley, Southern Tuscany, Italy based on multitemporal high-resolution terrestrial LiDAR and UAV surveys. *Geomorphology* **2016**, *269*, 8–22. [CrossRef]
35. D'Oleire-Oltmanns, S.; Marzolff, I.; Peter, K.D.; Ries, J.B.; Hssaïne, A.A. Monitoring soil erosion in the Souss basin, Morocco, with a multiscale object-based remote sensing approach using UAV and satellite data. In Proceedings of the 1st World Sustainability Forum, 1–30 November 2011; Available online: https://sciforum.net/paper/view/66c1c97e470ec89d5279ad7834155d28 (accessed on 25 January 2019). [CrossRef]
36. Pineux, N.; Lisein, J.; Swerts, G.; Bielders, C.L.; Lejeune, P.; Colinet, G.; Degré, A. Can DEM time series produced by UAV be used to quantify diffuse erosion in an agricultural watershed? *Geomorphology* **2016**, *280*, 122–136. [CrossRef]
37. Yang, Q. Study on Spatio-Temporal Distribution of Snow Cover in Northeast China and Its Simulation on Snowmelt Runoff. Ph.D. Thesis, Jilin University, Changchun, China, 2015.
38. Kothyari, U.C. Soil erosion and sediment yield modeling. *Ish J. Hydraul. Eng.* **2008**, *14*, 84–103. [CrossRef]
39. Zhang, T.J.; Barry, R.G.; Haeberli, W. Numerical simulations of the influence of the seasonal snow cover on the occurrence of permafrost at high latitudes. *Nor. Geogr. Tidsskr. Nor. J. Geogr.* **2001**, *55*, 261–266. [CrossRef]
40. Wang, E.H.; Zhao, Y.S.; Chen, X.W. Responses of soil structure to seasonal freezing-thawing in a typical black soil cultivated region. *Chin. J. Appl. Ecol.* **2010**, *21*, 1744–1750.
41. Carey, S.K.; Woo, M.K. Slope runoff processes and flow generation in a subarctic, subalpire catchment. *J. Hydrol.* **2011**, *253*, 110–129. [CrossRef]
42. Tarasova, L.; Basso, S.; Zink, M.; Merz, R. Exploring Controls on Rainfall-Runoff Events: 1. Time Series-Based Event Separation and Temporal Dynamics of Event Runoff Response in Germany. *Water Resour. Res.* **2018**, *54*, 7711–7732. [CrossRef]
43. Renard, K.G.; Foster, G.A.; Weesies, G.A.; McCool, D.K.; Yoder, D.C. *Predicting Soil Erosion by Water: A Guide to Conservation Planning with the Revised Universal Soil Loss Equation (RUSLE)*; Agricultural Handbook 703; US Department of Agriculture: Washington, DC, USA, 1997.
44. Poesen, J.; Nachtergaelea, J.; Verstraetena, G.; Valentinb, C. Gully erosion and environmental change: Importance and research needs. *Catena* **2003**, *50*, 91–133. [CrossRef]
45. Zhang, B.J.; Xiong, D.H.; Zhang, G.H. Impacts of headcut height on flow energy, sediment yield and surface landform during bank gully erosion processes in the Yuanmou Dry-hot Valley region, southwest China. *Earth Surf. Process. Landf.* **2018**, *43*, 2271–2282. [CrossRef]

46. Øygarden, L. Rill and gully development during an extreme winter runoff event in Norway. *Catena* **2003**, *50*, 217–242. [CrossRef]
47. Chow, T.L.; Rees, H.W.; Monteith, J. Seasonal distribution of runoff and soil loss under four tillage treatments in the upper St. John River valley New Brunswick, Canada. *Can. J. Soil Sci.* **2000**, *80*, 649–660. [CrossRef]
48. Sharratt, B.; Lindstrom, M.; Benoit, G.; Young, R.; Wilts, A. Runoff and soil erosion during spring thaw in the northern US Corn Belt. *J. Soil Water Conserv.* **2000**, *55*, 487–494.
49. Fan, H.; Wu, M.; Zhou, L.; Jia, Y. Study on sloping land snowmelt erosion affected by thaw depth of near-surface Meadow Soil. *J. Soil Water Conserv.* **2010**, *24*, 28–31.
50. Starkloff, T.; Hessel, R.; Stolte, J.; Ritsema, C. Catchment Hydrology during Winter and Spring and the Link to Soil Erosion: A Case Study in Norway. *Hydrology* **2017**, *4*, 15. [CrossRef]
51. Bowie, A.J. Investigations of vegetation for stabilizing eroding streambanks. *Trans. ASAE* **1982**, *25*, 1601–1606. [CrossRef]